



SIMULATION OF NEAR FIELD MIXING PROCESS IN MARINE DISPOSAL OF TREATED SEWER WATER

Akihiko Nakayama and Zafarullah Nizamani

Department of Environmental Engineering, Universiti Tunku Abdul Rahman, Jalan Universiti Bandar Kampar, Perak, Malaysia

E-Mail: akihiko@utar.edu.my

ABSTRACT

A numerical method of predicting the turbulent mixing process of a treated sewer disposed from a marine outfall is described. The momentum equations for the sea water mixed with treated water of small salinity and warmer temperature are solved numerically together with the equation of the concentration of the treated water. The basic method is a Large Eddy Simulation (LES) formulated on a fixed rectangular grid where boundaries are approximated by Immersed Boundary (IB) method. The sub-grid effects of the unresolved fluctuations of velocity and the concentration fields are expressed by the eddy viscosity and eddy diffusivity with the Smagorinsky model. The method is verified with an experiment and RANS calculation of the buoyant wall jet issuing on a solid surface. The method then is used to simulate the dispersion and dilution of the effluent from a typical marine outfall installed on the seabed of shallow coastal water. The behavior of the plume in the vicinity of the outfall is simulated well reproducing the dilution process and the surface boil. The results indicate that they can be used to estimate the effects of the outfall discharge on the water quality and the temperature in the near field to help design and determine a desirable treatment plant operation method.

Keywords: turbulent mixing, marine outfall, large eddy simulation, buoyant jet.

INTRODUCTION

It is important that the disposal of treated waste water is done properly anywhere, but is more so when it has to be done near a large city with many activities influenced by the quality and the temperature of sea water along the coast. While high water quality may be achieved by advanced treatment methods, the control of the temperature of the treated water is difficult and requires an expensive facility like a cooling pool. Therefore, an accurate estimate of the dispersion of the disposed water is required for the planning and operating a treatment plant.

There are a number of methods that may be used to predict the spread and dilution of the effluent concentration. A rough estimate may be made by using a method based on simple integral models (Blumeberg and Mellor, 1987). An estuary model (Nakatsuji *et al.*, 1992) or regional ocean simulation models such as CORMIX (Donecker and Jirka, 2007) and ROMS (Buijsman *et al.*, 2012) can also be used to obtain detailed distribution of contamination. These methods are based on the Reynolds-averaged equations of motion and the diffusion equation for contaminant transport that require appropriate turbulence models. Turbulence models in situations where the local fluid motion and mixing are influenced by such complicating factors as complex bathymetry with coastal structures and buoyancy due to salinity or temperature differences are not accurate or reliable. Also they are meant to predict the behavior of the dispersion in the far field after the effluent has spread to the full depth of the sea.

Large Eddy Simulation (LES) methods simulate the large-scale motion directly that are responsible for mixing and transports of the mixed fluid by modeling small-scale fluctuations and are more suited for dispersion calculations in complex geometry and boundary

conditions. The main problem is the large calculation loads. Here we apply an LES method with a wall model so the near field dispersion of contaminant concentration can be simulated with a computational grid of a reasonable size without resolving the viscosity influenced bottom layer. The detailed three dimensional distributions of the concentration and the temperature in the near field extending over a few hundred meters from the outfall can still be obtained. The results can be used for the purpose of evaluating the effects of the outfall effluent on the environment such as the marine life, coastal sea vegetable farming and the suitability of leisure facilities in the vicinity of the plant.

LES methods for simulating various flows are now available but the one that applies to flows with varying temperature and the density in open seas is not. It is stressed that detailed and accurate distributions of the concentration of the mixed treated water need to be obtained including the vertical variations.

In the following, first the basic equations to simulate the motion of seawater mixed with fresh water of small salinity and different temperature are described in the framework of the large eddy simulation with the necessary models. Then a brief description of the numerical method used to solve them is given. The method is validated in calculation of a basic buoyant plume before applying to an outfall dispersion in real case.

GOVERNING EQUATIONS AND NUMERICAL METHOD

The basic equations we solve are the spatially-filtered equations of motion with Boussinesq approximation with Coriolis's terms



$$\frac{\partial u_i}{\partial t} + \frac{\partial(u_i u_j)}{\partial x_j} + 2\varepsilon_{ijk}\Omega_j u_k = -\frac{1}{\rho_0} \frac{\partial p}{\partial x_i} + \nu \frac{\partial^2 u_i}{\partial x_j \partial x_j} - \delta_{i3}(\beta(T - T_0) + \zeta(C - C_0))g - \frac{\partial \tau_{ij}}{\partial x_j} \quad (1)$$

$$\frac{\partial u_i}{\partial x_i} = 0 \quad (2)$$

- x_i = Cartesian coordinates with x_3 (which may be designated by z) vertically upward
 u_i = velocity component in x_i direction,
 p = filtered pressure
 T = filtered temperature
 C = filtered concentration
 Ω_j = earth's rotation vector,
 ρ_0 = ambient water density
 T_0 = ambient temperature
 C_0 = ambient concentration of treated water
 ν = coefficient of the kinematic viscosity
 β = coefficient of thermal expansion of water due to changes of temperature
 ζ = coefficient of density changes of water due to changes of concentration of treated water
 g = acceleration due to gravity
 τ_{ij} = sub-grid stress components

The sub-grid stress τ_{ij} in the present calculation is modeled by the standard Smagorinsky model

$$\tau_{ij} = \nu_{sgs} \left(\frac{\partial u_i}{\partial x_j} + \frac{\partial u_j}{\partial x_i} \right) \quad (3)$$

$$\nu_{sgs} = (C_S \Delta)^2 \left| 2 \left(\frac{\partial u_i}{\partial x_j} + \frac{\partial u_j}{\partial x_i} \right) \left(\frac{\partial u_i}{\partial x_j} + \frac{\partial u_j}{\partial x_i} \right) \right|^{1/2} \quad (4)$$

- ν_{sgs} = Sub-grid eddy viscosity
 C_S = 0.11 Smagorinsky constant,
 Δ = average grid spacing

More elaborate models that may perform better than the standard Smagorinsky model, may be used but it can be studied if any insufficiency of the present approach becomes apparent.

The boundary conditions to be used for these equations make use of the wall similarity law for the solid wall boundary condition. In other words, the shear stress on solid walls is calculated by the following model equation and is used in the momentum equation instead of using (3).

$$\tau_{ij} = C_d \rho V_1 u_{ij1} \quad (5)$$

- V_1 = total velocity $\sqrt{u_1^2 + v_1^2 + w_1^2}$,
 C_d = resistance coefficient,
 $(\cdot)_1$ = value at calculation point closest to solid wall
 u_{ij} = Tangential velocity component in x_j direction

Subscript 1 means the value at the computational point closest to the solid wall. The resistance coefficient C_d is determined from the standard wall similarity law for smooth or rough surfaces using V_1 and the distance from the wall y_1 . This way the no-slip velocity condition, which is a poor approximation for high Reynolds number flows with coarse grid, is not used. This is important since the simulation will be conducted for flows with the dimensions of the real coastal water.

The equations for the filtered water temperature T and the filtered concentration C of the treated water are

$$\frac{\partial T}{\partial t} + \frac{\partial(Tu_j)}{\partial x_j} = \alpha \frac{\partial^2 T}{\partial x_j \partial x_j} - \frac{\partial q_j}{\partial x_j} \quad (6)$$

$$\frac{\partial C}{\partial t} + \frac{\partial(Cu_j)}{\partial x_j} = \gamma \frac{\partial^2 C}{\partial x_j \partial x_j} - \frac{\partial h_j}{\partial x_j} \quad (7)$$

- α = coefficient of the heat conduction of water
 γ = coefficient of the concentration diffusion
 q_j = sub-grid scale heat flux
 h_j = sub-grid scale concentration flux

The sub-grid heat flux and the sub-grid concentration flux are modeled by the sub-grid eddy diffusivity model with the eddy diffusivity coefficient determined by an extension of the Smagorinsky model.

$$q_j = \frac{\nu_{sgs}}{\sigma_{sgs}} \frac{\partial T}{\partial x_j}, \quad (8)$$

$$h_j = \frac{\nu_{sgs}}{\sigma_{sgs}} \frac{\partial C}{\partial x_j}, \quad (9)$$

The value of the sub-grid diffusion Prandtl number σ_{sgs} in these equations are assumed to be constant 0.7 and no modification for the effects of stratification are used since the large eddies that are likely to be influenced by the buoyancy are directly calculated in LES.

The water surface is expressed by its elevation h as a function of the horizontal coordinates (x_1, x_2) or (x, y). It is determined by solving the spatially-filtered kinematic boundary condition at the free surface

$$\frac{\partial h}{\partial t} + \frac{\partial(hu_{s1})}{\partial x_1} + \frac{\partial(hu_{s2})}{\partial x_2} = u_{s3} + \frac{\partial \tau_{hx}}{\partial x_1} + \frac{\partial \tau_{hy}}{\partial x_2} \quad (10)$$

where (u_{s1}, u_{s2}, u_{s3}) are the velocity components on the free surface and τ_{hx}, τ_{hy} are the sub-grid free-surface fluctuation terms (Hodges and Street, 1999), which we model by the gradient model (Yokojima and Nakayama, 2002).

The detailed description of the numerical method of solution used here is given in Nakayama (2012). It is based on the HSMAC algorithm (Hirt and Cook, 1972) and the pressure is solved iteratively so that the continuity equation is satisfied. For the cells containing the free surface, the free surface height is determined from Eq. (9)



and the pressure is set to the atmospheric pressure instead of solving for the pressure using the continuity equation. The spatial derivative terms are all evaluated by the central difference formula. Time advancing is done by the third-order Adams-Bashforth method. The method applying the boundary condition is also described in the accompanying paper. For the boundary conditions of the temperature T and concentration C , the immersed boundary method is used.

VERIFICATION BY CALCULATION OF BUOYANT WALL JET

The present method is validated by calculating the basic dispersion problem of hot water injected into ambient still cold water. The hot water jet is issued horizontally through a circular tube of negligible wall thickness placed on the bottom floor of a mixing basin as shown in Figure-1.

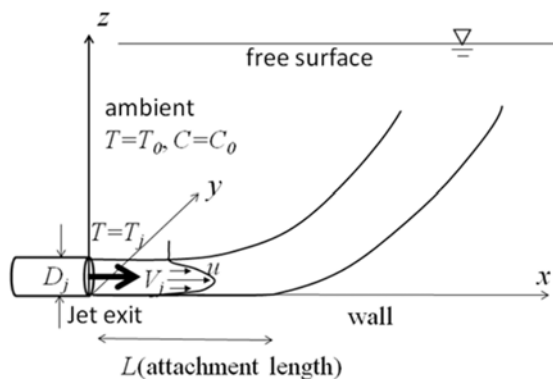


Figure-1. Buoyant jet issuing from a circular pipe on a wall.

Table-1. Parameters in two calculation cases. (values of L are the results of the calculation.).

Case	D_j (mm)	V_j (mm/s)	T_j (deg)	T_0 (deg)	F_d	Re_j	L/D_j
Case1	4.7	1.0	80	20	37.7	10086	119
Case2	4.7	1.75	90	20	44.2	26111	149

The temperature and the density of the issuing water are T_j and D_j , respectively. The mean velocity of the jet at the exit is V_j . The diameter of this jet is D_j and the temperature and the density of the ambient water are T_0 and ρ_0 , respectively. The depth of the water in the experiment is large compared with the jet diameter and the free surface condition is not needed. The rest of the calculation conditions are taken the same as the experiment of Sharp and Vyas (1977) and the numerical calculation by Huai *et al.* (2010) and are summarized in Table-1. The Reynolds number Re_d indicated in the table is defined by D_j , V_j and the kinematic viscosity which is

assumed to be constant. The Froude number F_d is defined by

$$F_d = V_j / \sqrt{g D_j (\rho_0 - \rho_j) / \rho_j} \quad (11)$$

L shown at the right most column of the table and shown in Figure-1 is the attachment length defined by the horizontal distance from the jet exit to the point where the temperature dilution ratio becomes equal to 0.03 on the wall.

$$S = (T - T_0) / (T_j - T_0) \quad (12)$$

Calculations for two cases with different Reynolds and Froude numbers are conducted. In these validation cases, the density is a sole function of the temperature and the concentration C of the jet fluid does not directly influence the flow.

In the numerical calculation, a rectangular grid of constant spacing is used. The grid spacing in the horizontal directions is 2mm and that in the vertical direction is 1mm, so the jet exit cross section is represented by 4 x 2 cells. Due to this crude representation of the exit cross section, the volume discharge rate rather than the point-wise velocity is set to correspond to the experiment. The total of 79 x 67 x 82 grid points are used to cover the region of 160 diameters in the horizontal direction and $30D_j$ in the depth direction. The horizontal distance in the direction of the jet is sufficiently large so the boundary condition at the right boundary does not influence the plume trajectory.

The calculation results are shown in Figure-2 through Figure-5. Figure-2 shows the velocity distribution in two planes perpendicular to the jet axis in the near field close to the exit. They verify the velocity calculation by comparing with Verhoff's theoretical solution.

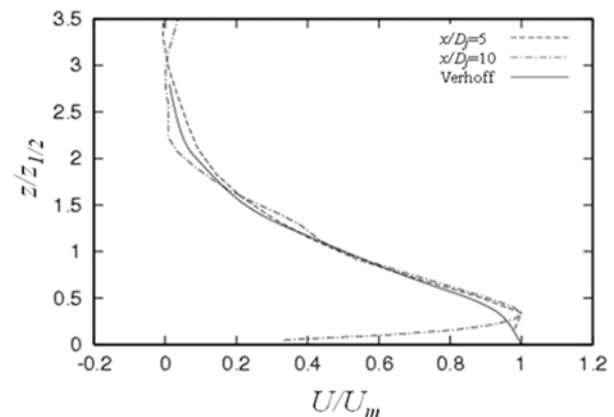


Figure-2. Calculated velocity distributions near the exit of the wall jet compared with the theoretical profile of Verhoff.

The velocity is normalized by the average velocity U_m across the jet cross section and plotted against normalized height $z/z_{1/2}$, where $z_{1/2}$ is the height where the



velocity is one half of the maximum. The shape of the distribution above the near wall layer agrees with Verhof's profile. The Verhof used the inviscid assumption and the velocity is made to have zero slope on the wall which is not realistic. In the present calculation, the wall model based on the wall similarity is used which reduces to the laminar boundary layer at sufficiently low Reynolds number, and the velocity drops near the wall. The value on the wall itself is not computed but is seen to approach zero.

Figure-3 shows the calculated attachment length L of the two calculation cases compared with the experiments of Sharp and Vyas (2007) and the Reynolds-Averaged Navier-Stokes (RANS) calculation of Huai *et al.* (2010). It is seen that the calculation results are slightly smaller than the experiment but the trend agrees with the mean of the experimental values.

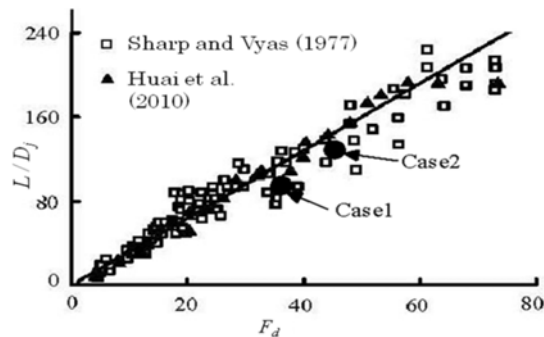


Figure-3. The calculated attachment length compared with experiments.

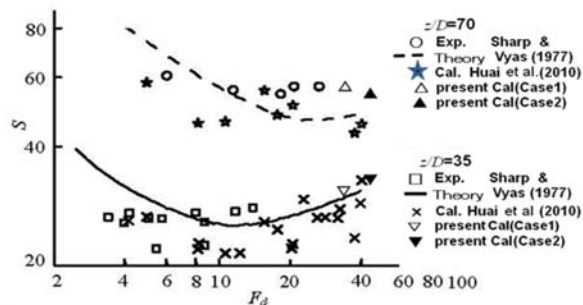


Figure-4. The calculated temperature dilution at $z/D_j = 35$ and 70 compared with experiments.

Figure-4 is the minimum temperature dilution in the planes $z/D_j = 35$ and 70 from the two calculation results. They are compared with the experimental data and the RANS calculation of Huai *et al.* (2010). The present results are only near the high end of the Froude number range of the experimental data but are seen to agree with them and the RANS calculation.

Figure-5 is a snapshot of instantaneous distributions of the velocity vectors and the temperature in the vertical plane through the jet axis. The upper right

inset is the enlarged view near the exit. The way the buoyant effluent billows up is seen to be reproduced well.

The above results indicate the present method does simulate buoyant plumes of the configuration and the buoyancy similar to the typical marine disposal of treated water.

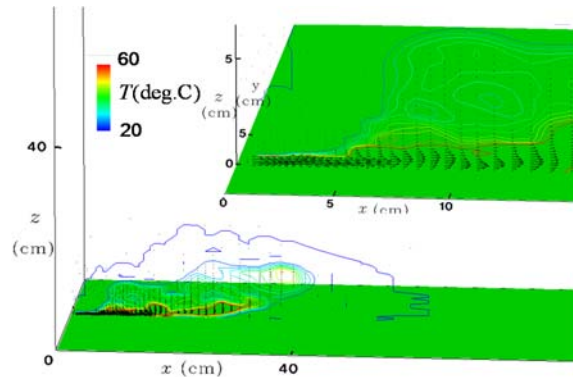


Figure-5. The instantaneous velocity and temperature distributions. Upper right inset is the enlarged view near the jet exit.

CALCULATION OF INITIAL MIXING OF EFFLUENT FROM REAL OUTFALL ON SEABED

The above described LES method is now applied to calculation of dispersion from a typical outfall located near a coast.

Figure-6 shows a numerical representation of a coastal water zone where a water treatment plant is located above the ground behind the seawalls. An underground pipe runs from the bottom of the plant transporting the treated water to the seabed where the outfall ports are installed. The average depth of the water is 12m and the location of the outfall is 50m offshore from the seawalls. We simulate the initial mixing and spread of the treated water discharged from 6 nozzles directed in the horizontal direction. The objective is to obtain the detailed concentration variation of the treated water and the temperature rises in the vicinity of the plant. It is assumed that there are tidal currents with varying velocity and direction depending on the tidal phase.

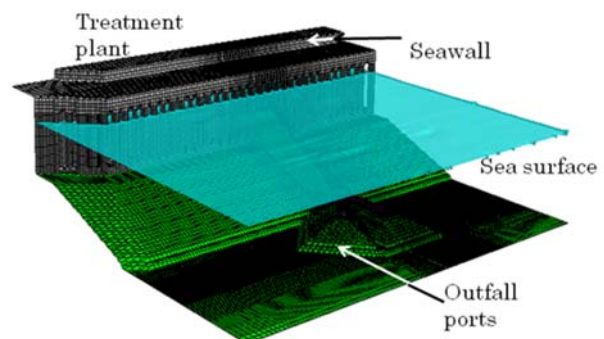


Figure-6. Water treatment plant outfall on seabed on a coast.

**Table-2.** Calculation cases and conditions of diffusion of treated water from submarine outfall.

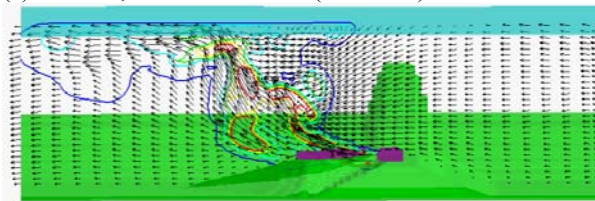
Case	tidal current m/s	no. of outfall ports	discharge rate m ³ /s	seawater salinity psu	sea water temperature °C	treated water temperature °C
CaseA	-0.2	6	1.0	30.0	18.0	20.0
CaseB	0.2					
CaseC	-0.2		2.0			

The computational grid is rectangular as in the validation case, but the grid spacing in the horizontal directions is now variable. The smallest horizontal spacing is 25cm near the outfall ports and 4m at the outer boundaries. The vertical grid spacing is 10cm with 48 grids in the vertical directions. The calculation region is 700m x 1000m x 15m in the offshore, alongshore and depth directions, respectively covered by 182 x 214 x 48 grid points. The outlet nozzle cross section of the outfall port is resolved by 2 x 2 cells.

The boundary condition on the sea bed and on the solid structures is as described in the previous section. The boundary conditions on the outer boundary are the partially-clamped radiation condition on the velocity and the water elevation formulated by Blumberg and Kantha (1985).

Table-2 summarizes the calculation conditions that are typical of treatment plants of moderate cities and discharge rate of 1m³/s and 2m³/s are assumed. The temperature of the treated water is warmer in most seasons and two degrees above the sea water is assumed. Tidal currents can exist in real situations and eastward and westward currents of 0.2m/s average velocity are assumed.

(a) Case A, westward current (to the left)



(b) Case B, eastward current (to the right)

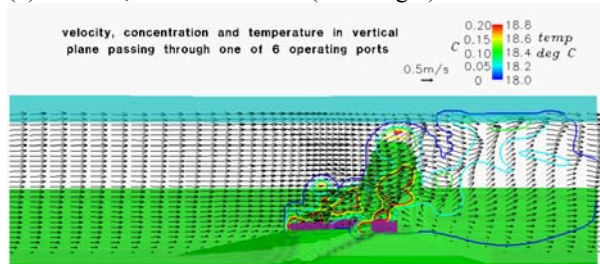
**Figure-7.** Velocity, temperature and concentration distributions in a vertical plane near the outfall.

Figure-7 shows the instantaneous flow and the temperature fields for the Case A and Case B with two different current directions in a vertical plane passing through the center of the outfall ports. The vertical scale of these figures is enlarged by five times of the horizontal scale for easy view of the shallow flow area. Figure-6(a) is the case when the tidal current is in the direction of the outfall nozzles and Figure-7(b) is the case when the current opposes the direction of the outfall. In both cases, the treated water has initial salinity zero and the temperature 2.0 degrees higher than the sea water. The plume rises within a short distance from the outfall ports and forms a boil on the sea surface. After the plume reaches the surface it rapidly spreads in the horizontal directions. It is what usually is observed at the sites of in shallow disposals.

Figure-8 is the view from the top of Case B in which the current opposes the outfall direction. The gray shaded area is the plume with the concentration larger than 1 percent. The position and the size of the plume intersecting the sea surface resemble the observation at a plant in Japan (Bricker *et al.*, 2006). Figure-9 shows a photograph of the sea surface near the outfall. The smooth surface indicating a boil of the outfall effluent is seen. While it is not an indication of the quantitative verification, the plume behaviour close to the outfall is reproduced correctly at least qualitatively. More quantitative comparisons are underway.

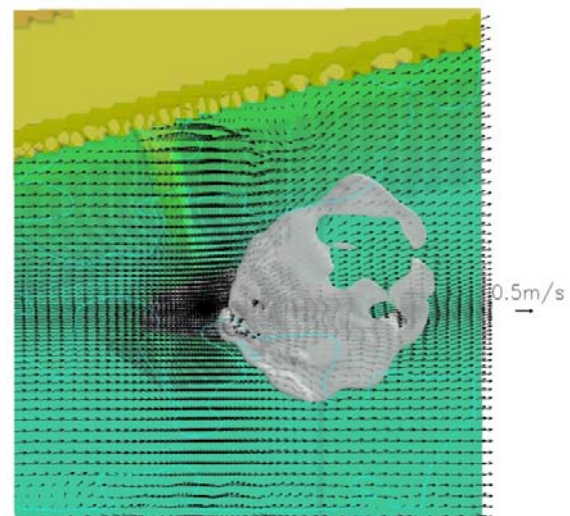
**Figure-8.** Top view of the surface boil in case B. The gray surface is the surface of constant concentration of 1 percent.



Figure-9. View of the sea surface showing the boil above outfall at a plant in Japan (Bricker *et al.*, 2006).

CONCLUSIONS

The large eddy simulation method based on the filtered equations of Boussinesq approximated equations of motion for the treated water mixed in the ambient sea water has been developed. After it is validated in the calculation of basic buoyant jets it is applied to simulate the dispersal of a model case of a treated water marine disposal. It does not make hydrostatic or other approximations and resolve the turbulent motion responsible for the mixing processes and is able to simulate the detailed mixing and dispersal processes in the region close to the outfall. Although there is a limitation on the extent of the simulation region and the duration of the simulation period, it can be improved as the computer performance is improved. The present method can be an alternative to integral methods that make drastic assumptions like Gaussian distribution.

REFERENCES

- [1] Blumberg, A. F. and Kantha, I. H. (1985). Open boundary condition for circulation models, *J. Hydraul. Eng.*, 111(2), pp.237-255.
- [2] Blumberg, A. F. and Mellor, G. L. (1987). A description of a three-dimensional coastal ocean circulation model. *Three-Dimensional Coastal Ocean Models*. Ed., N. S. Heaps, Vol. 4, Coastal and Estuarine Sciences, Amer. Geophys. Union, pp.1-16.
- [3] Bricker, D.J., Nakayama, A. Aoki, C. and Takada, M. (2006). Plume tracing in the coastal area with strong tidal currents, *JSCE Journal of Coastal Engineering*, 53, pp.346-350.
- [4] Buijsman, M., Uchiyama, Y., McWilliams, J.C. and Hill-Lindsay, C.R. (2012). Modeling semidiurnal internal tides in the Southern California Bight, *J. Phys. Oceanogr.*, 42, pp.62-77.
- [5] Donecker, R.L. and Jirka, G.H. (2007). CORMIX User Manual: A Hydrodynamic Mixing Zone Model and Decision Support System for Pollutant Discharges into Surface Waters, EPA-823-K-07-001.
- [6] Frick, W.E., Roberts, P.J.W., Davis, L.R., Keyes, J., Baumgartner, J. and George, K.P. (2003). *Dilution models for effluent discharges*, 4th ed., U.S. Environmental Protection Agency, Washington.
- [7] Hirt, C.W. and Cook, J.L. (1972). Calculating three-dimensional flow around structure and over rough terrain. *J. Comput. Phys.* 10, pp.324-340.
- [8] Hodges, B.R. and Street, L. R. (1999). On simulation of turbulent nonlinear free-surface flows, *J. Comp. Phys.* 151, pp.425-457.
- [9] Huai, W.-X., Li, Z.-W., Qian, Z.-D., Zeng, Y. and Hann, J. (2010). Numerical simulation of horizontal buoyant wall jet, *Journal of Hydrodynamics*, 22(1), pp.58-65.
- [10] Nakatsuji, K., Yamami, H., Sueyoshi, T. and Fujiwara, T. (1992). Numerical study of the residual current in Osaka Bay, *JSCE Journal of Coastal Engineering*, 39, pp.906-910.
- [11] Nakayama, A. (2012). Large-eddy simulation method for flows in rivers and coasts constructed on a cartesian grid system. *Memoirs of Construction Engineering Research Institute*, 54(papers), pp.13-27.
- [12] Sharp, J. J. and Vyas, B.D. (1977). The buoyant wall jet, *Proc. Instn. Civ. Engrs. (London)*, 63(2), pp.593-611.
- [13] Yokojima, S. and Nakayama, A. (2002). Filtering effects of freesurface fluctuations in LES of open-channel turbulent flows. *Annu. J. Hydraulic Engng. JSCE* 46, pp.379-384.